Article:
Yelland, T.S., Daood, S.S. and Nimmo, W. (2021) Comparing fuel additives for fireside corrosion inhibition in pulverised fuel boilers using thermodynamic modelling. Calphad, 74. 102283. ISSN: 0364-5916

https://doi.org/10.1016/j.calphad.2021.102283

Comparing Fuel Additives for Fireside Corrosion Inhibition in Pulverised Fuel Boilers Using Thermodynamic Modelling

Thomas S. Yelland [a], Syed Sheraz Daood [b,c], William Nimmo [a]

[a] Energy 2050, Energy Engineering Group, Department of Mechanical Engineering, University of Sheffield, Sheffield, S10 2TN, United Kingdom.

[b] Institute of Energy and Environmental Engineering, University of the Punjab, Lahore, Pakistan.

[c] Energy Engineering Research and Development Centre, Faculty of Electrical, Energy & Environmental Engineering, University of the Punjab, Lahore, Pakistan.

Keywords: Fireside corrosion; additive; biomass; thermodynamic modelling; chemistry

Corresponding Author: sdaood.icet@pu.edu.pk

ABSTRACT

This study presents a method for comparing corrosion inhibiting fuel additives using the thermodynamic modelling softwate FactSage^{TM}. Two biomass ashes were investigated while using a range of loadings of three additives: Fe-based additive and two coal ashes, one with an 80% Si and Al contents and one with less than 50% of Si and Al contents but having a significant Ca content. The metrics used for analysis were the formation of various corrosive compounds and by-products. The Fe-based additive could inhibit the formation of corrosive species but not as well as either of the coal ashes, as it was key to increase the Si and Al content of the deposits. The coal ash with the greatest Si and Al content proved most capable of inhibiting fireside corrosion, while the contaminants present in the other coal ash proved detrimental to reducing the production of certain corrosive species. This method can be used as a qualitative predictive tool by research and development teams to quickly and economically understand the consequences of utilising fuel additives on ash chemistry or of changes in proportion/sources of fuel in a power plant.

1. INTRODUCTION

Fireside corrosion of superheater and reheater tubes is a major issue within pulverised fuel boilers that can lead to downtime and the need to replace the tubes [1]. In order to reduce CO_2 emissions, biomass is likely to become the solid fuel of choice in pulverised fuel systems. This will exacerbate fireside corrosion due to the increased alkali metal and chlorine content in the fuel. Fireside corrosion can arise primarily from the reaction of sulphur and chlorine based compounds in the fly ash deposit and the flue gas with the metal tubing.

Sulphur dioxide and trioxide from the flue gas can react with either metal iron or iron and alkali oxides in the fly ash deposit to form iron or alkali sulphates, the precursors to the formation of the highly corrosive and eutectic compound alkali iron trisulphate [2-4]. The formation of this molten compound can result in the removal of the protective iron oxide layer, laying bare the base iron and allowing oxidation and sulphation, thus creating a cycle [2]. Further to this, a second cycle will be created when the alkali iron trisulphates react with the base metal, forming iron sulphide (Eq. 1-3), which can then be oxidised to reform SO_2 [5].

$$3A_2SO_4 + Fe_2O_3 + 3SO_3 \rightarrow 2A_3Fe(SO_4)_3 \quad (1)$$

$$Fe_2O_3 + 3SO_3 \leftrightarrow Fe_2(SO_4)_3 \quad (2)$$

$$9Fe + 2A_3Fe(SO_4)_3 \rightarrow 3A_2SO_4 + 4Fe_2O_3 + 3FeS \quad (3)$$

Alternatively, it has been reported that alkali sulphates, after reacting with SO_3, form alkali pyrosulphates, which can then react with iron and the protective iron oxide layer (Eq. 4-7) [6].

$$SO_2 + \frac{1}{2}O_2 \rightarrow SO_3 \quad (4)$$

$$A_2SO_4 + SO_3 \rightarrow A_2S_2O_7 \quad (5)$$

$$3A_2S_2O_7 + Fe_2O_3 \rightarrow 2A_3Fe(SO_4)_3 \quad (6)$$

$$3A_2S_2O_7 + 3Fe \rightarrow Fe_2O_3 + FeS + A_2SO_4 \quad (7)$$

Chlorine in the flue gas mostly exists as Cl_2, HCl and alkali chlorides. HCl can react with the protective metal oxide layer and the base metal to form $FeCl_2$; HCl can also be oxidised to form Cl_2, which will also react with the base metal to form iron chloride (Eq. 8-10).

$$2HCl + FeO \rightarrow FeCl_2 + H_2O \quad (8)$$

$$2HCl + Fe \rightarrow FeCl_2 + H_2 \quad (9)$$

$$Cl_2 + Fe \rightarrow FeCl_{2(s)} \rightarrow FeCl_{2(g)} \quad (10)$$

The iron chloride then vaporises and can be entrained in the flue gas and carried out of the boiler or oxidised to form iron oxide and Cl_2, thus creating a chlorination cycle (Eq. 11) [7].

$$FeCl_{2(g)} + \frac{3}{2}O_2 \rightarrow Fe_2O_3 + Cl_2 \quad (11)$$

Alkali chlorides, although primarily linked to ash deposition, can act as the primary conveyor of chlorine to the scale and metal surfaces; where, they can condense and react with metal oxides and SO_2 to form alkali sulphates and Cl_2, enabling further corrosive processes (Eq. 12-13) [8-9].

$$2ACl_{(s,l)} + Fe_2O_3 + \frac{1}{2}O_2 \rightarrow A_2Fe_2O_4 + Cl_2 \quad (12)$$

$$2ACl + SO_2 + O_2 \rightarrow A_2SO_4 + Cl_2 \quad (13)$$

A burgeoning technique for minimising the rate of ash based fireside corrosion is the use of fuel additives, a series of minerals or chemicals that alter the chemistry of the ash in order to abate ash-related problems via four well established mechanisms: chemical absorption, physical adsorption, disruption of ash melting and ash dilution [10]. The chemical absorption involves alkali vapours and melts being captured by the additive, forming stable compounds with far higher melting temperatures. Physical adsorption involves sequestering of vapours within highly porous particulates, which are then removed from the boiler. Ash melting can be disrupted through the reduction of the temperature range or the increase in melting temperature that can be

achieved by the introduction of inert materials. In literature [10] fuel additives are divided into four groups based on the most active component: potassium based additives, sulphur based additives, calcium based additives and aluminium/silicon based additives (including alumino-silicates). Potassium based additives can react with potassium to form potassium phosphates, thereby reducing the amount of potassium available for corrosion reactions [11]. Calcium based additives introduce calcium that can dissolve in potassium silicates, ejecting the potassium into the gas phase and creating calcium silicates with higher melting temperatures [12]. Sulphur based additives are used to convert KCl to K_2SO4, which has a higher melting temperature and releases chlorine into the flue gas, minimising chlorination of the base metal [13-14]. Aluminium and silicon based additives consist of alumino-silicates, such as kaolin, and silica and alumina rich mixes, such as coal ash [15-16]; both react with KCl to form $K_2O{\cdot}Al_2O_3{\cdot}xSiO_2$ and $KAlO_2$ respectively, while the silica and alumina rich mixes are generally considered to be less efficient and less capable than alumino-silicates [17-18].

Rarely discussed in the context of corrosion abatement are Fe-based additives. Initial studies show their ability improve coal combustion by increasing combustion efficiency, reducing carbon in ash and reducing NO emissions [19-20]. While later studies also found an interaction with ammonia when Fe-based additives were utilised during selective non-catalytic reduction [21]. More prominently, the Fe-based additive was shown to reduce the corrosivity of coal ash, thought to be through the interruption of alkali iron tri-sulphate formation processes or the interruption of base metal chlorination by excess iron oxide in the additive [4]; although, iron oxide is also known to react with KCl to form $K_2Fe_2O_4$ and Cl_2 [22]. Furthermore, the addition of Fe_2O_3 to ash has been found to have a negative impact on the ash melting processes [23]. Therefore, it can be concluded that there are benefits to using a Fe-based additive but there is a lack of clarity as to which mechanisms, as listed prior, are the cause of any benefits.

For predicting ash behaviour within real boilers, laboratory data can prove difficult to utilise; therefore, equilibrium modelling can be used instead as the full composition of the ash and flue gas are taken into account [24]. This technique has played a leading part or even the sole basis in a multitude of important studies covering fireside corrosion [8, 25-26], biomass ash challenges [27-28] and additives [23, 29-30].

The aim of this study is to investigate the impact of an Fe-based additive on fireside corrosion caused by solid fuel ashes and compare the impact with that of possible economical alternatives, two coal fly ash of varying composition. Moreover, power stations co-fire, primarily, biomass fuels (agricultural wastes, such as sunflower husks/peanut shells, and energy crops) with coal fly ash that has a high unburned carbon content. Hence, by means of equilibrium modelling, this work aims to provide confidence and clarity regarding these additive and specific configuration technologies in order to aid in their development. This study also presents an economical and quick method for use by plant research and operational team to assess the potential impact of additives in inhibiting fireside corrosion.

2. METHOD

The thermodynamic equilibrium modelling software FactSage^{TM} was used to investigate theoretical ash deposits. This proprietary software contains thermodynamic databases with thousands of pure substance compounds and hundreds of evaluated and optimised metal oxide and molten and solid salt solutions, as well as many other solutions not applicable in this case [31]. The FactSage^{TM} 'Equilib' module utilises these databases to model complex multi-phase equilibria using the Gibb's free energy minimisation technique. The limitations to the utilisation of the FactSage^{TM} databases have been well discussed in the study [9]. These limitations include: the lack of influence of kinetic constraints, residence times and temperature/concentration gradients; a lack of consideration of physical processes; an assumption of perfect mixing; and the results are completely dependent on the input variables and the selected databases. Measures

to minimise the impact of these limitations have been discussed [9] but, simplified, any model requires careful consideration and full disclosure of input conditions and solution selection in order to grant the ability to compare and contrast with alternative and experimental results.

Table 1 – Compositions of the ashes

	Peanut Shell Ash (%) (Rizvi, 2015)[24]	Standard deviation based on peanut shell ash samples	Sunflower Husk Ash (%) (Rizvi, 2015) [24]	Standard deviation based on sunflower husk ash samples
SiO_2	35.51	0.49	3.21	0.05
TiO_2	0.83	0.01	0.03	0.00
Al_2O_3	8.25	0.11	0.48	0.01
Fe_2O_3	3.24	0.04	0.84	0.01
MgO	5.16	0.07	15.24	0.21
CaO	9.29	0.13	27.16	0.38
Na_2O	1.33	0.02	0.21	0.00
K_2O	31.10	0.43	45.10	0.64
P_2O_5	4.52	0.06	5.30	0.07
SO_3	0.78	0.01	2.43	0.03
Cl	0.01	0.00	-	-

The focus of this investigation is to study the corrosive potential of ash deposits with varying loadings of fuel additives on stainless steel tubing of a furnace. The selection of the solutions, discussed later, allows for the monitoring of the production of species that are either responsible for the initiation of corrosive processes or are by-products of this corrosion. The yield of these species act as metrics representing corrosive potential of an ash deposit and any changes in these yields indicate an impact of the addition of additive to the tested ash deposits. The results of the calculations are not expected to give exact verifiable yields but rather provide trends and information regarding the probability of these additive to impede corrosion under the investigated ash deposit.

The tested biomass fuels were derived from literature [24] represent a range of fuels in terms of their silica, alumina and potassium contents. The ash contents are displayed in Table 1. The composition of the Fe-based additive [4, 19-20] was derived from the study [19] by taking an average of all the individual components and then normalising the mixture. A second additive,

that will be referred to as the Ca-rich coal ash, was tested in conjunction with the Fe-based additive; this was chosen in order to compare the effects of the Fe-based additive with the effects of an additive that would be low cost, has a high silica content and is likely to be used for reasons other than corrosion inhibition, such as increasing heat transfer performance in industrial boilers. The Ca-rich coal ash contains significant impurities, which may impact its effectiveness, namely the calcium oxide and sulphur components. Kaolin is widely discussed in literature as being a choice additive for corrosion inhibition [10] but costs approximately 210 USD/ton compared to 8 USD/ton of coal fly ash [32]. It would be preferable to utilise a coal ash that resembles kaolin in having a high concentration of alumina and silica and without significant levels of impurities. Such an 'Al-rich' coal ash can be found in the study [4] and will be compared to the Ca-rich coal ash in order to highlight the importance of the presence of impurities and to discuss to what degree 'any' coal ash can be used in biomass boilers. The compositions of the additives are shown in Table 2.

Table 2 – Compositions of the additives

	Fe-based Additive (%) (Daood, et al, 2014) [18]	Standard deviation based on Fe-additive	Ca-rich coal ash (CA) (%)	Standard deviation based on Ca-rich additive	Al-rich CA (%) (Daood, et al., 2017) [21]	Standard deviation based on Al-rich additive
SiO_2	38.04	0.21	31.87	0.18	56.28	0.31
TiO_2	0.20	0.001	0.50	0.003	1.04	0.01
Al_2O_3	4.60	0.03	15.88	0.09	23.38	0.13
Fe_2O_3	49.24	0.27	8.59	0.05	6.62	0.04
MgO	1.44	0.01	2.20	0.01	2.10	0.01
CaO	3.94	0.02	18.28	0.10	6.31	0.03
Na_2O	0.79	0.004	2.00	0.01	0.37	0.002
K_2O	0.64	0.004	0.70	0.004	2.19	0.01
P_2O_5	0.44	0.002	0.40	0.002	0.58	0.003
SO_3	0.67	0.004	19.58	0.11	1.13	0.01

Reactants were inputted into the module so that each model contained flue gas from the combustion of 1 kg of the respective fuel with an excess air of 18% typical for a combustion chamber (the compositions of which are shown in Table 3), 5 g of T22 steel (the composition of which is shown in Table 4) and 100 g of accumulated ash deposit.

Four additive fuel loadings were investigated (0%, 1.5%, 5.5%, 8%); 0% being chosen in order to set a baseline behaviour and 1.5% being chosen in order to investigate any transitionary behaviour between 0% and 5.5%. Ash mixtures were calculated by combining the masses of the individual ash components within 1 kg of each fuel with the masses of the individual additive components needed to load the fuel to the specified loading. A temperature range was chosen in order to simulate the possible temperature range witnessed in an ash deposit, from 400ºC at the tube wall to 900ºC in the flue gas in steps of 10ºC (Figure 1), while the step change was chosen so as to not to omit any results that may have a short but pivotal formation temperature window.

Table 3 – Composition of the flue gas for each fuel

	Peanut Shell	Sunflower Husk
CO_2 (g)	1555.40	1644.28
H_2O (g)	530.82	547.02
N_2 (g)	4518.06	4852.41
O_2 (g)	209.48	224.89
SO_2 (g)	3.32	2.19
HCl[a] (g)	1.08	1.44

[a] Based on typical flue gas values

Table 4 – Composition (% wt.) of T22 Steel [33]

	C	Si	Mn	P	S	Cr	Mo	Fe
T22	0.05-0.15	≤0.50	0.30-0.60	≤0.025	≤0.025	1.90-2.60	0.87-1.13	Bal.

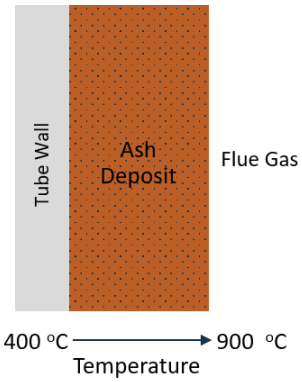

Figure 1 – Potential temperature gradient within an ash deposit on a tube wall

This study utilises four databases within FactSage™:

- FactPS, a collection of data related to pure substances,
- FToxid, a collection of pure oxides and oxide solutions, including various slag solutions,
- FTsalt, a collection of pure salts and salt solutions,
- FTpulp, a database designed for the paper and pulp industry but very applicable to solid fuel combustion due to the collection of sodium and potassium compounds (including chlorides, sulphates and pyrosulphates).

Four solutions are used:

- FTpulp-MeltB, containing liquid phase alkali salts, hence simulating corrosive melt formations,
- FTpulp-Hexa, containing solid phase alkali sulphates, carbonates and sulphides (this solution must be dilute in sulphides and high temperature to be valid),
- FTpulp-ACl, containing solid phase alkali chlorides (with dissolved alkali hydroxides),
- FTpulp-OrtB, a low temperature solid phase solution of alkali sulphates and carbonates requiring a high concentration of K_2SO_4.

3. RESULTS

3.1. A Comparison of Fe-based Additive, Ca-rich Coal Ash and Al-rich Coal Ash Addition to Peanut Shell Ash

Figure 2 presents the impact of various loadings of Fe-based additive, Ca-rich coal ash and Al-rich coal ash on the yield of gaseous KCl and $FeCl_2$ from a peanut shell ash deposit. The three additives appear to have a definite impact on KCl yield. The Ca-rich coal ash appears to have a far greater impact at each additive loading in comparison to the Fe-based additive; in addition, the Fe-based additive required a loading of 5.5% to have a significant impact on the KCl yield, whereas the Ca-rich coal ash was shown to be beneficial at only 1.5%. Also of note, is the fact that the temperature, at which the additives were starting to decrease the KCl yield, decreased as the additive loading increased.

The Al-rich coal ash can be observed to be far more proficient at reducing KCl yield than the Ca-rich coal ash at all loadings except 1.5%, where there is little deviation from the baseline. Most interestingly for the uptake of this technology, the Al-rich coal ash is capable of dramatically reducing KCl yield across the entire temperature range when a loading of 8% is used. As for the $FeCl_2$ yield, all cases greatly deviate from the baseline except the 1.5% Al-rich coal ash case, mirroring the lack of impact that this loading causes. The fact that the other cases are grouped together, even though a varying amount of potassium has been captured, indicates a maximum rate for the iron chlorination cycle within this deposit was reached. It stands to reason that if the $FeCl_2$ is unable to rise any further, it would be desirable to maximise potassium capture, safe in the knowledge that the excess chlorine will most likely be entrained in the flue gas and removed.

The mechanism for KCl capture by coal ash is well understood [10] and is due to the significant Al_2O_3 and SiO_2 concentrations in the coal ash leading to reactions with either silicates or alumino-silicates. However, the addition of the Fe-based additive does not greatly increase the

alumina concentration in the deposit. Therefore, the reasons for the decreased KCl yield are either due to dilution, a separate interaction with KCl, the catalysis of the alumino-silicate reactions by the iron oxide or the preferential chlorination of iron oxide over potassium oxide. Although, dilution is unlikely to be the sole cause of the decrease in yield due to the far greater decrease in KCl than K_2O.

Furthermore, the decreased KCl for each case is accompanied by a substantial increase in $FeCl_2$ production from the peanut ash deposit, with a significant increase regardless of which additive is used and an increasing rise in $FeCl_2$ production with additive loading; this implies that the drop in KCl arises from chemical absorption that results in HCl liberation. However, the increase in $FeCl_2$ between 1.5% and 8% Ca-rich coal ash is far smaller than the respective increase when using the Fe-based additive, even though more KCl is being captured. It stands to reason that this is either due to the far greater Fe_2O_3 content in the Fe-based additive loaded deposit, aiding the increased $FeCl_2$ formation, or, as seen in literature, that the increased CaO content of the Ca-rich coal ash loaded deposit is leading to neutralisation reactions with the liberated HCl [30] via Eq. (14).

$$CaO + 2HCl \rightarrow CaCl_2 + H_2O \quad (14)$$

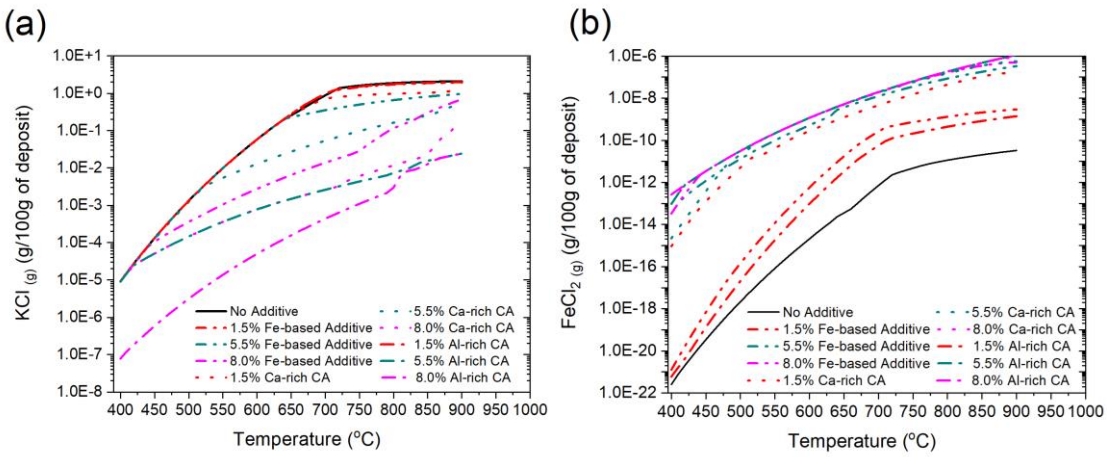

Figure 2 – The impact of loading of the Fe-based additive, Ca-rich coal ash and Al-rich coal ash on the yield of gaseous (a) KCl and (b) $FeCl_2$ from a peanut shell ash/flue gas mixture across the working temperature range

It should also be mentioned that the rise in $FeCl_2$ compared to the baseline case is significant but orders of magnitude smaller than the fall in KCl, hence implying that the $FeCl_2$ increase is an acceptable side effect.

Figure 3 presents the impact of the Fe-based additive, Ca-rich coal ash and Al-based coal ash on the yield and formative temperature range of corrosive liquid salts from a peanut shell ash deposit. Loading the deposit with increasing amounts of Fe-based additive narrows the temperature window at which the corrosive liquid salts can form dramatically, until these liquid salts are eliminated at 5.5% loading. Use of the Ca-rich coal ash or the Al-rich coal ash at 1.5% loading, although positive, does not have as big an impact as the Fe-based additive on the temperature window; however, a 5.5% loading of either coal ash was also found to prevent liquid salt formation. The new temperature range during the use of the Al-rich coal ash is higher than its Ca-rich coal ash counterpart, which may prove useful if a plant is utilising older boilers working with steam at lower temperatures. With regard to the yield of liquid KCl and K_2SO_4, yield decreases with respect to the baseline case when 1.5% Fe-based additive loading is used and falls further when the equivalent amount of Ca-rich coal ash is utilised; while, addition of 1.5% Al-rich coal ash only provides minor improvement to the yield of liquid KCl and K_2SO_4 compared to the baseline case.

Peculiarly, the yield of the liquid pyrosulphate increases dramatically for each case, showing greater formation with the use of the Ca-rich coal ash over the Fe-based additive and the Al-rich coal ash. This is likely a side-effect of the capture of K_2SO_4, which will lead to a release of SO_3 and SO_2 that will react with remaining K_2SO_4 to produce potassium pyrosulphate. Formation of these pyrosulphates are suggested by several authors [34-35], but only a few cases with analytical evidence have been reported [36-37]. The pyrosulphate formation reactions have been shown in

Eq. (4-5). The alkali pyrosulphates have been reported to be potential precursors in the formation of alkali-iron tri-sulphates that have relatively low melting points [36].

The formative temperature range of pyrosulphates, especially in the liquid phase, is reported to be from 380°C to less than 900°C, depending upon the concentration of SO_3 [34-35, 38]. Whereas in this study, the reported formation temperature range of liquid salts is from 650°C to less than 700°C. It should also be noted that the Ca-rich coal ash also has a high sulphur content already reported to increase the pyrosulphate yield [35, 38]. This leads to a several orders of magnitude rise in the formation of this troublesome compound; however, the yield is still very low compared to the other prominent corrosive liquid salts, a also reported in [34].

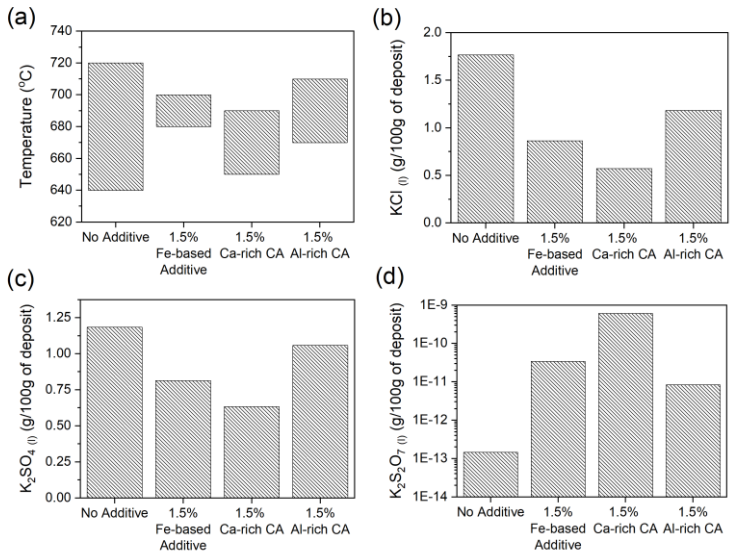

Figure 3 – The impact of loading of the Fe-based additive, Ca-rich coal ash and the Al-rich coal ash on the yield of liquid salts and the formative temperature range in a peanut shell ash/flue gas mixtures.

Figure 4a presents the impact of the Fe-based additive, Ca-rich coal ash and Al-rich coal ash on the yield and formative temperature range of solid KCl from a peanut shell ash deposit. The decreased formative temperature range of the liquid salt solution during the use of 1.5% Fe-based additive has the impact of increasing the temperature range where solid KCl is present; however, the yield compared to the baseline is lower from 500°C to 640°C. As the Fe-based additive loading is increased further to 5.5%, the yield decreases substantially and the formative

temperature range is the same as the baseline case. Increasing the loading further to 8% decreases the yield even further and shrinks the temperature range immensely so that the KCl no longer forms above 450°C. However, there are periods at which the Fe-based additive performs marginally better at certain periods, such as 400-480°C for the 5.5% loading.

The Al-rich coal ash only has a slight positive impact on yield when 1.5% loading is used, while the increased temperature range, compared to the baseline, is due to the shifted and contracted temperature range of the liquid solution. Both the yield and the temperature range greatly improve with an increase in Al-rich coal ash loading. The 5.5% Al-rich coal ash case behaves as effectively as the 8% Ca-rich coal ash case and any further increase in loading leads to the elimination of the solid solution.

In terms of contextualising these observations, the presence of oxides of Al and Si present in additives have been reported to bind alkali compounds in relatively inert silicates [34]. The Ca-rich coal ash performs slightly better at each loading, with yield and temperature range decreasing steadily with each increase in loading. Furthermore, the utilisation of Ca-based additives to develop high-melting silicates composed of calcium and alkali metals was reported to be the main factor in increasing corrosion resistance of the studied steels [10, 34].

Very visible kinks are seen in the lines for the 1.5% Ca-rich coal ash case and the 5.5% Fe-based additive case at 520°C and 570°C respectively. These occur at the same point as the phase transition between the potassium sulphate containing OrtB and Hexa solutions, and these kinks are most likely a consequence of this, as it becomes energetically favourable for some potassium to be sulphated rather than chlorinated.

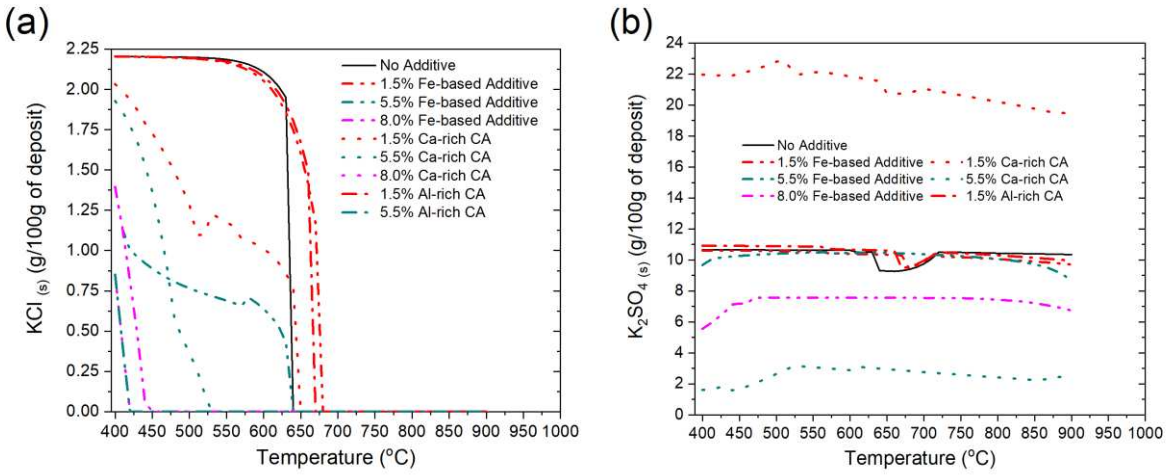

Figure 4 – The impact of loading of the Fe-based additive and the Ca-rich coal ash on the yield of solid (a) KCl and (b) K_2SO_4 in a peanut shell ash/flue gas mixture

Figure 4b presents the impact of the Fe-based additive and the Ca-rich coal ash on the yield and formative temperature range of solid K_2SO_4 from a peanut shell ash deposit. The addition of the Fe-based additive leads to marginal improvements in K_2SO_4 yield with increasing loading, the rate of which implies that it is most likely a result of potassium dilution. The Ca-rich coal ash, on the other hand, intensifies the formation of K_2SO_4 greatly at 1.5% loading; improvements are only witnessed once the loading has been increased to 5.5% but at this point, the K_2SO_4 yield is far less than even the 8% Fe-based additive case. These initial increases may be a result of the relatively sizeable SO_3 content in the Ca-rich coal ash and the comparative lack of potassium dilution at these loadings. This can be seen as a warning over the use of additives containing sulphur; the resulting increase in K_2SO_4, especially when it is as great as seen during the 1.5% case, may cause more damage than it prevents from the conversion of KCl to K_2SO_4. It has been experimentally reported that the KCl sulphation reaction, originating from the addition of an additive with a high sulphur content, facilitates in the production of solid K_2SO_4 [38-40]. When the loading is increased to 8%, the solid solution is eliminated altogether. Unlike the Ca-rich coal ash, the 1.5% Al-rich coal ash case produces a yield similar to the baseline, rather than significantly greater. Further to this, any additional increase in Al-rich coal ash loading leads to

the elimination of the solid solution, thus eliminating corrosion reaction pathways originating from alkali sulphates and, hence, reducing overall corrosion rates associated with this ash.

In a separate study, the cross sectional images of alloys exposed to air conditions at a temperature different to this study (1000ºC) reported higher corrosion rates for high Fe_2O_3 concentration cases and decreased alkali sulphate formation in the case, where oxides of Al and Si were present in additives [41]. Similarly, the use of a silicon-aluminium fly ash, with a similar composition to the Al-rich coal ash used in this study, reported a noticeable improvement in the ash fusion temperatures and subsequent corrosion related issues. When the fly ash ratio reached 9%, the mixed ash was mainly composed of plagioclase and quartz; this is ascribed to the high level of Al_2O_3 in the ash that reacted with SiO_2 and available CaO from the fuel and additive [42].

3.2 A Comparison of Fe-based Additive, Ca-rich Coal Ash and Al-rich Coal Ash Addition to Sunflower Husk Ash

Figure 5 presents the impact of various loadings of Fe-based additive, Ca-rich coal ash and Al-rich coal ash on the yield of gaseous KCl and $FeCl_2$ from a sunflower husk ash deposit. This ash, when no additive is being used, contains the greatest amount of potassium out of those tested; that being noted, this ash is also arguably the least impacted by either of the additives. Not until 5.5% loading of Ca-rich coal ash is the KCl yield significantly impacted, and increasing the loading further does not lead to any considerable improvement. The Al-rich coal ash performs similarly, except from ~450°C to ~700°C, where the 8% Al-rich coal ash case performs better than the equivalent Fe-based additive and Ca-rich coal ash cases. The lack of disparity in the trends from each additive may be related to the fact that the sunflower husk ash has the highest initial potassium concentration; therefore, once potassium is sequestered by an alumino-silicate, more KCl may be formed by the chlorination of the present excess potassium. This phenomenon would seem to require a sufficiently large native potassium content and may also be used to explain the relative lack of impact by the lower additive loadings on KCl yield from the other

biomass ashes. The above results can also be indirectly compared with the findings from a study, where an increased proportion of blended fuels led to a higher K fraction that impacted ash deposit related corrosion [43].

The $FeCl_2$ yield trends mirror the KCl trends well in that the greatest deviation from the baseline occurs for the 5.5% and 8% loadings of the Ca-rich coal ash and the Al-rich coal ash; although, the 5.5% and 8% loadings of Fe-based additive do also lead to significantly greater $FeCl_2$ yield without presenting any considerable reduction in KCl. The yield of $FeCl_2$ from the 8% Al-rich coal ash case exceeds the other cases across a similar temperature window to the KCl divergence, due to the sequestering of potassium, leading to the liberation of chlorine and greater $FeCl_2$ formation.

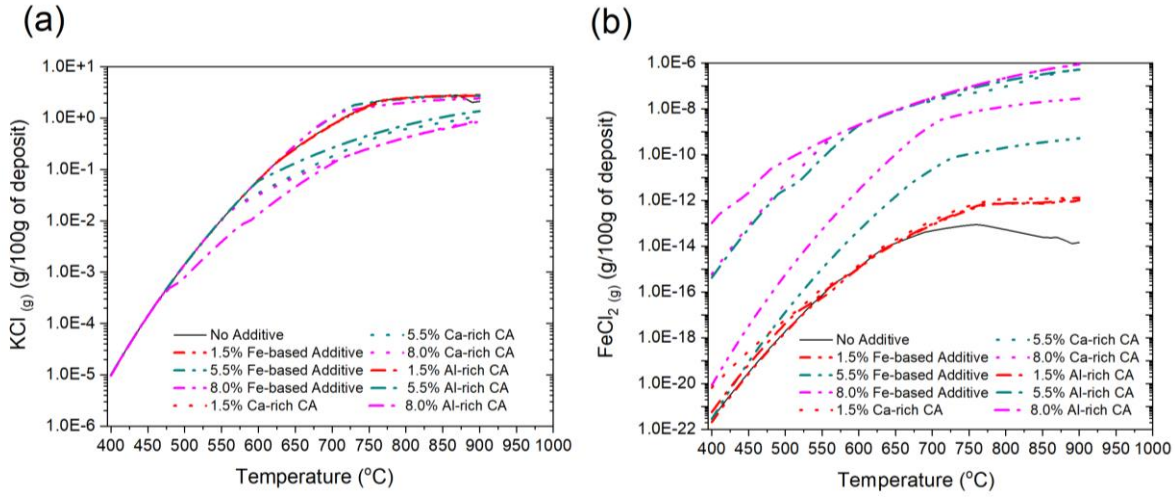

Figure 5 –The impact of loading of the Fe-based additive, Ca-rich coal ash and Al-rich coal ash on the yield of gaseous (a) KCl and (b) $FeCl_2$ from a sunflower husk ash/flue gas mixture across the working temperature range.

Figure 6 presents the impact of the Fe-based additive, Ca-rich coal ash and Al-based coal ash on the yield and formative temperature range of corrosive liquid salts from a sunflower husk ash deposit. In contrast to the impact on the gaseous KCl, Fe based additives have a positive impact on the formative temperature range of corrosive liquid salts within the deposit. Increasing the loading of the Fe-based additive narrows the temperature range dramatically from 130°C for the

baseline case to 20°C for the 8% loading case. In literature, a shift in the melting temperature of the formed salts was also reported when a higher calcium content additive and a coal fly ash were used as additives [10, 44]. In comparison, the Ca-rich coal ash and the Al-rich coal ash prove even more effective, eliminating the formation of the deposit altogether at a loading greater than 1.5%.

As for the yield of the liquid KCl, there is not much impact in utilising either additive until the loading is at least 5.5%; although, when 8% Fe-based additive is utilised, the yield of liquid KCl is less than half the baseline case. The impact of the additives on the yield of liquid K_2SO_4 is less clear. The yield increases from the baseline as loading of the Ca-rich coal ash is increased, while the introduction of the Fe-based additive initially decreases the yield when loading is 1.5% but as the loading is increased to 5.5%, there is a large increase in yield. From here on, the yield decreases as loading is increased but 8% Fe-based additive is required to fall below the baseline level again.

The Al-rich coal ash has an impact of slightly decreasing the yield of liquid K_2SO_4 at a loading of 1.5%. Though it is difficult to find relevant benchmarking measures, the silicon-aluminium additives have the capability of capturing alkali metals especially when there is a high SiO_2 content. As with the peanut shell ash, the use of the additives increases the yield of potassium pyrosulphate (Fig. 3d), with the Ca-rich coal ash causing the greatest increase in yield at 1.5% but the Fe-based additive causing further increases in yield with increasing loading. Eq. (4-6) chemical reactions specifies conversion of potassium and sulphur to K_2SO_4 and SO_3 catalysed in presence of iron to produce pyrosulphates [34], particularly when potassium and sulphur are in larger concentrations in the tested fuel ash.

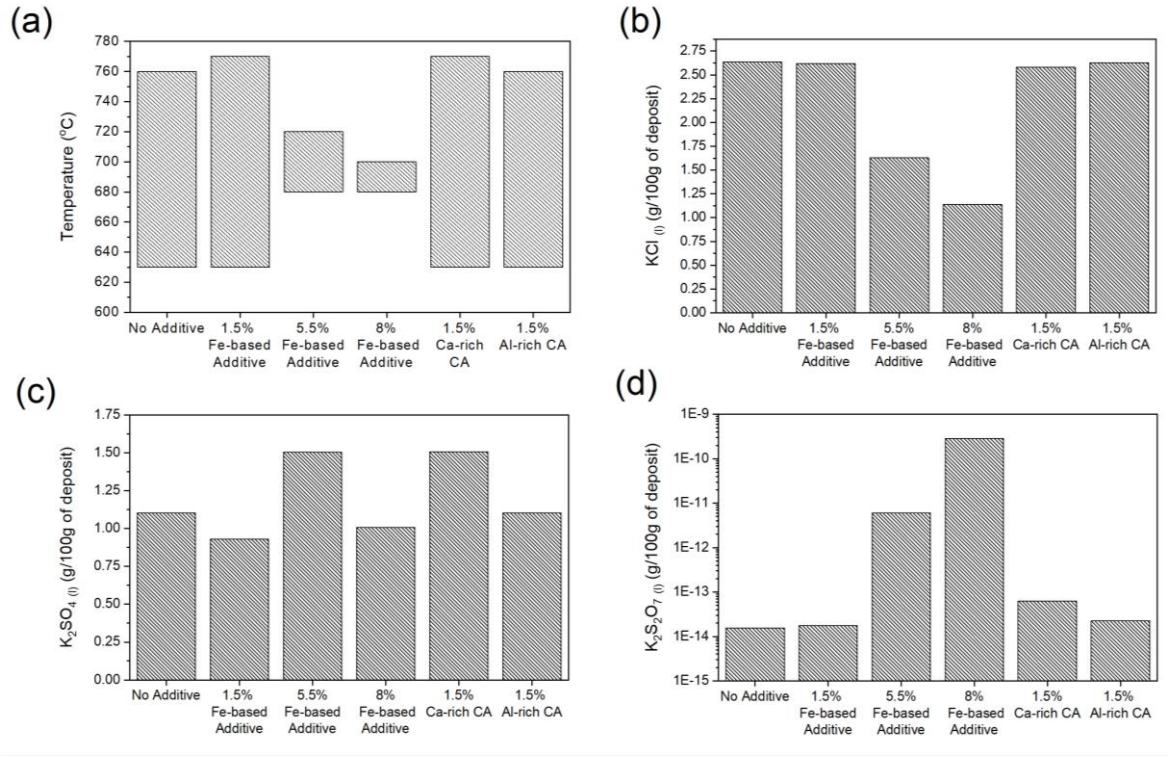

Figure 6 – The impact of loading of the Fe-based additive, Ca-rich coal ash and the Al-rich coal ash on the yield of liquid salts and the formative temperature range in a sunflower husk ash/flue gas mixture.

Figure 7a presents the impact of the Fe-based additive, Ca-rich coal ash and Al-rich coal ash on the yield and formative temperature range of solid KCl from a sunflower husk ash deposit. Introducing the Fe-based additive results in a slight decrease in yield that grows with increasing loading. The formative temperature range changes with the changing initial melt temperature witnessed in Figure 6. The Ca-rich coal ash has a minor impact on yield when the loading is 1.5%, although this decrease in yield is greater than any of the Fe-based additive cases from 400-550°C. Increasing the loading to 5.5% decreases the yield substantially, while also decreasing the formative temperature range by ~100°C. There is no great benefit to increasing the loading of Ca-rich coal ash further than 5.5% for this ash. The 1.5% Al-rich coal ash case only presents a minor improvement to the baseline case; while increasing the loading of Al-rich coal ash to 5.5% will decrease the yield and the temperature range but to less of an extent as the equivalent Ca-rich coal ash case. However, increasing the loading of Al-rich coal ash to 8% produces a

much reduced yield (over 50% reduction) and a decrease in end temperature, 480°C compared to 570°C for the 8% Ca-rich coal ash and 630°C for the baseline.

Figure 7b presents the impact of the Fe-based additive, Ca-rich coal ash and Al-rich coal ash on the yield and formative temperature range of solid K_2SO_4 from a sunflower husk ash deposit. As with the peanut shell ash, the Fe-based additive has a slight positive impact on K_2SO_4 yield, with the yield decreasing by smaller rates as the loading is increased. The impact of the Ca-rich coal ash is erratic. At first, there is a rise in solid K_2SO_4 yield with increasing loading, with the maximum yield being witnessed at 3% Ca-rich coal ash. Increasing loading further leads to a decrease in yield, but not even during the 8% loading case does the yield fall below the baseline. The issue of the significant SO_3 content in the Ca-rich coal ash is far more noteworthy with an increased native potassium content. Each Al-rich coal ash case performs better than the baseline, with performance improving as loading increases and the 8% loading case proving able to substantially reduce the yield and the temperature range, so that solid K_2SO_4 only forms from 710-820°C, which may prove vital for plants using an older generation of boiler.

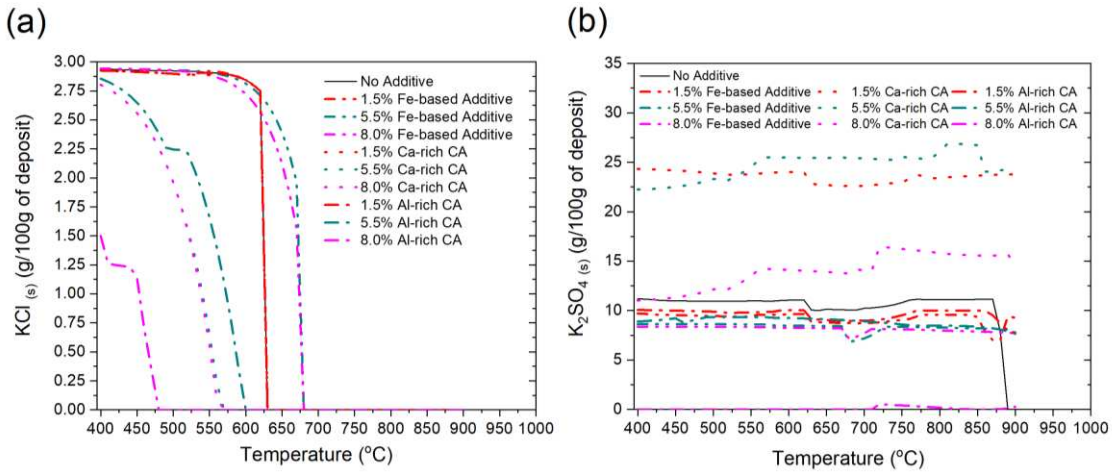

Figure 7 – The impact of loading of the Fe-based additive and the Ca-rich coal ash on the yield of solid (a) KCl and (b) K_2SO_4 in a peanut shell ash/flue gas mixture

3.3. Further discussion

In literature, FactSage^{TM} thermodynamic equilibrium modelling used for slag formation and corrosion assessments have reasonably predicted the changes of gas, solid and liquid phases during pure and co-combustion configurations [9,45]. Comparable early-stage investigations, although with some limitations, still offer the benefit of pre-screening the most important conditions to be set up in real experimental environments, so as to be an essential starting point for experiments [9]. Nevertheless, experimental investigations can also require costly and time-intensive resources with occasional inconclusive findings [9, 24, 46] from the complex to set-up testing facilities, i.e. simulated fireside corrosion setup [4, 34], boiler fireside deposits retrieval system [35], and so forth. It is difficult to quantify the difference between modelling and experimental approaches, however, in qualitative terms, a test on simulated fireside corrosion setup requires over 1000 hours of operation to produce deposits on boiler tube sections, which is substantially greater than the time required to set up a variety of cases on FactSage^{TM}.

FactSage^{TM} calculations helped to predict phase formations with the changing temperature and chemical composition of investigated additives. This study frames the investigation in the context of an ash deposit on a wall tube, with the temperature range being investigated as an assumption of the temperature gradient through this ash deposit. In this context, the baseline cases show that significant $KCl_{(g)}$ concentrations exist at the upper end of the temperature range, hence most likely closer to the gas-ash interface as opposed to the metal surface. Therefore, the action of these additives capturing this $KCl_{(g)}$ and releasing free chlorine is unlikely to cause great chlorination at the metal surface or the protective oxide layer and the measured increase in $FeCl_2$ is likely to instead originate from the chlorination of the loose iron oxide in the deposit. Furthermore, if this free chlorine is released close to the gas-ash interface, then there is a likelihood that this could be entrained in the flue gas and carried out of the boiler, hence meaning that the $FeCl_2$ predictions in the upper end of the temperature range may be overestimations. It is also prevalent to consider that these models only consider that reactions start within the

deposit, but in actuality there may be a large portion of potassium captured prior to the deposition; further to this, the capturing of potassium prior to deposition may also reduce the amount and speed of deposition occurring.

With regard to corrosive melts, the baseline results show that melts tend to from 600-800 C; this could prove to be an issue when supercritical and ultra-supercritical systems are installed in order to maximise efficiency and subsequently the superheater temperature increases. The increased temperature will make it more likely that the ash melt will come in contact with the protective metal oxide, or even the wall itself, and will exacerbate corrosion rates. Therefore, it is necessary to utilise an additive when more advanced steam systems are implemented in order to reduce the impact of any increase in corrosion. An aspect of this implementation, which has been overlooked in this study for brevity, is the impact on fouling and slagging processes within these boilers; purely due to the increased ash mass within the boiler alone, it is possible that these processes may be aggravated. However, further computational work could be done to assess this.

Although this is a capable means of analysing the corrosive potential of ash deposits, weaknesses in the context of the results should be discussed. One key weakness is the absence of alkali iron trisulphate formation reactions within the databases. In order to approximate the damage caused by these compounds, the formation of the precursors to this compound must instead be analysed; however, this is will not be a perfect alternative as any interaction that hinders the formation of alkali iron trisulphates from these precursor compounds is not acknowledged. The fact the input mixture is perfectly mixed is also slightly problematic as this eliminates any concentration gradient that may be present in a practical scenario; furthermore, the sulphur dioxide and hydrogen chloride can have direct contact with the steel in this case, as opposed to the ash deposits acting as a physical barrier in a practical scenario.

4. CONCLUSIONS

This study aims to investigate the impact of commercial additives on fireside corrosion of superheater tubes during biomass combustion using equilibrium modelling to assess the changes in yield of corrosive compounds as an ash deposit's composition is altered by the presence of additives. This study also presents this method as a qualitative predictive tool that can be used to quickly and economically analyse how ash chemistry may change in the presence of additives. The additives under investigation were an Fe-based additive and two coal ashes, with varying contents. The ashes under investigation were peanut shell ash and sunflower husk ash, representing decreasing silica content and increasing potassium content. This study resulted in the following noteworthy findings:

- The Fe-based additive was able to consistently reduce the gaseous KCl yield when used with the peanut shell ash, but was not effective with this metric when used with the sunflower husk ash. The liquid solution was prevented from forming at 5.5% loading during use with the peanut shell, but could only reduce the temperature range with the sunflower husk ash. Inhibition of the solid phase KCl required 5.5% loading for the peanut shell ash, but could not be achieved for the sunflower husk ash. The solid phase K_2SO_4 could only be impacted via dilution when using the Fe-based additive. The information presented here most likely does not warrant the use of the Fe-based additive for the purpose of inhibiting fireside corrosion alone, but it will most likely have some positive impact on reducing fireside corrosion if used for NO_x abatement at a loading of 5.5% or higher.
- The Ca-rich coal ash is evidently more proficient at inhibiting fireside corrosion than the Fe-based additive, as expected. The Ca-rich coal ash performed well with both ashes, requiring a loading of 5.5% to have a significant impact on most metrics, with exception to the yield of solid K_2SO_4 from the sunflower husk ash, which was severely aggravated

by the addition of any Ca-rich coal ash. This highlights the importance of understanding the impact of any contaminants in the added coal ash as the Ca-rich coal ash had a considerable sulphur content. For the sunflower husk ash, the potassium content was so considerable that the combination of reduced dilution (compared to other additives) and introducing more sulphur resulted in the yield of solid phase K_2SO_4 being unable to drop below the baseline values.

- The Al-rich coal ash proved far better at reducing yields than the Ca-rich coal ash, but in some cases required a greater loading than the Ca-rich coal ash to start to have an impact. The Al-rich coal ash proved particularly capable at eliminating the solid phase KCl and K_2SO_4 yield when 8% loading was used with the peanut shell ash, and all but eliminating them when 8% loading was used with the sunflower husk ash.

The trends presented here should encourage an operator to, if possible, use coal ash with the greatest Si and Al content or, at the very least, encourage an operator that there is value in knowing the composition of an added coal ash. While, the method and metrics shown here can be utilised by operators in order to quickly and economically predict the impact of available corrosion inhibiting additives.

REFERENCES

[1] N.J. Simms, J. Sumner, T. Hussain, J.E. Oakey, Fireside issues in advanced power generation systems, Mater. Sci. Technol. 29 (2013) 804-812. https://doi.org/10.1179/1743284712Y.0000000133.

[2] J.N. Harb, E.E. Smith, Fireside corrosion in PC-fired boilers, Prog. Energy Combust. Sci. 16 (1990) 169-190. https://doi.org/10.1016/0360-1285(90)90048-8.

[3] J. Tomeczek, Corrosion modelling of austenitic steel in molten sulphate deposit, Corros. Sci. 49 (2007) 1862-1868. https://doi.org/10.1016/j.corsci.2006.10.012.

[4] S.S. Daood, M. Ottolini, S. Taylor, O. Ogunyinka, Md.M. Hossain, G. Lu, Y. Yan, W. Nimmo, Pollutant and corrosion control technology and efficient coal combustion, Energy Fuels 31 (2017) 5581-5596. https://doi.org/10.1021/acs.energyfuels.7b00017.

[5] W.T. Reid, External Corrosion and Deposits: Boiler and Gas Turbines, American Elsevier Publishing, New York, 1971.

[6] A. Hendry, D.J. Lees, Corrosion of austenitic steels in molten sulphate deposits, Corros. Sci. 20 (1980) 383-404. https://doi.org/10.1016/0010-938X(80)90007-4.

[7] H.J. Grabke, E. Reese, M. Spiegel, The effects of chlorides, hydrogen chloride and sulphur dioxide in the oxidation of steels below deposts, Corros. Sci. 37 (1995) 1023-1043. https://doi.org/10.1016/0010-938X(95)00011-8.

[8] Y. Zeng, K. Li, R. Hughes, J.L. Luo, Corrosion mechanisms and materials selection for the construction of flue gas component in advanced heat and power systems, Ind. Eng. Chem. Res. 56 (2017) 14141-14154. https://doi.org/10.1021/acs.iecr.7b03664.

[9] M. Becidan, L. Sorum, F. Frandsen, A.J. Pedersen, Corrosion in waste-fired boilers: A thermodynamic study, Fuel 88 (2009) 595-604. https://doi.org/10.1016/j.fuel.2008.10.032.

[10] L. Wang, J.E. Hustad, O. Skreiberg, G. Skjevrak, M. Gronli, A critical review on additives to reduce ash related operation problems in biomass combustion applications, Energy Procedia 20 (2012) 20-29. https://doi.org/10.1016/j.egypro.2012.03.004.

[11] A. Grimm, N. Skoglund, D. Bostrom, M. Ohman, Bed agglomeration characteristics in fluidised quartz bed combustion of phosphorus-rich biomass fuels, Energy Fuels 25 (2011) 937-947. https://doi.org/10.1021/ef101451e.

[12] P. Thy, C.E. Lesher, B.M. Jenkins, Experimental determination of high-temperature elemental losses from biomass slag, Fuel 79 (2000) 693-700. https://doi.org/10.1016/S0016-2361(99)00195-7.

[13] M. Aho, P. Vainikka, R. Taipale, P. Yrjas, Effective new chemicals to prevent corrosion due to chlorine in power plant superheaters, Fuel 87 (2008) 647-654. https://doi.org/10.1016/j.fuel.2007.05.033.

[14] M. Brostrom, H. Kassman, A. Helgesson, M. Berg, A. Andersson, R. Backman, A. Nordin, Sulfation of corrosive alkali chlorides by ammonium sulfate in a biomass fired CFB boiler, Fuel Process. Technol. 88 (2007) 1171-1177. https://doi.org/10.1016/j.fuproc.2007.06.023

[15] H. Wu, M.S. Bashir, P.A. Jensen, B. Sander, P. Glarborg, Impact of coal fly ash addition on ash transformation and deposition in a full-scale wood suspension-firing boiler, Fuel 113 (2013) 632–643. https://doi.org/10.1016/j.fuel.2013.06.018.

[16] L.J. Roberts, P.E. Mason, J.M. Jones, W.F. Gale, A. Williams, C. Ellul, Investigating the impact of an Al-Si additive on the resistivity of biomass ashes, Fuel Process. Technol. 178 (2018) 13-23. https://doi.org/10.1016/j.fuproc.2018.05.018.

[17] M.J. Fernandez Llorente, P. Diaz Arocas, L. Gutierrez Nebot, J.E. Carrasco Garcia, The effect of the addition of chemical materials on the sintering of biomass ash, Fuel 87 (2008) 2651-2658. https://doi.org/ 10.1016/j.fuel.2008.02.019.

[18] S. Kyi, B.L. Chadwick, Screening of potential mineral additives for use as fouling preventatives in Victorian brown coal combustion, Fuel 78 (1999) 845-855. https://doi.org/10.1016/S0016-2361(98)00205-1.

[19] S.S. Daood, G. Ord, T. Wilkinson, W. Nimmo, Fuel additive technology – NOx reduction, combustion efficiency and fly ash improvement for coal fired power stations, Fuel 134 (2014) 293-306. https://doi.org/10.1016/j.fuel.2014.04.032.

[20] S.S. Daood, G. Ord, T. Wilkinson, W. Nimmo, Investigation of the influence of metallic fuel improvers on coal combustion/pyrolysis, Energy Fuels 28 (2014) 1515-1523. https://doi.org/10.1021/ef402213f.

[21] S.S. Daood, T.S. Yelland, W. Nimmo, Selective non-catalytic reduction – Fe-based additive hybrid technology, Fuel 208 (2017) 353-362. https://doi.org/10.1016/j.fuel.2017.07.019.

[22] M. Montgomery, T. Vilhelmsen, S.A. Jensen, Potential high temperature corrosion problems due to co-firing of biomass and fossil fuels, Mater. Corros. 59 (2008) 783-793. https://doi.org/10.1002/maco.200804166.

[23] H. Zhou, J. Wang, B. Zhou, Effect of five different additives on the sintering behaviour of coal ash rich in sodium under an oxy-fuel combustion atmosphere, Energy Fuels 29 (2015) 5519-5533. https://doi.org/10.1021/acs.energyfuels.5b00500.

[24] T. Rizvi, P. Xing, M. Pourkashanian, L.I. Darvell, J.M. Jones, W. Nimmo, Prediction of biomass ash fusion behaviour by the use of detailed characterisation methods coupled with thermodynamic analysis, Fuel 141 (2015) 275-284. https://doi.org/10.1016/j.fuel.2014.10.021.

[25] I. Ja'baz, F. Jiao, X. Wu, D. Yu, Y. Ninomiya, L. Zhang, Influence of gaseous SO_2 and sulphate-bearing ash deposits on the high-temperature corrosion of heat exchanger tube during oxy-fuel combustion, Fuel Process. Technol. 167 (2017) 193-204. https://doi.org/10.1016/j.fuproc.2017.06.033.

[26] M. Paneru, G. Stein-Brzozowska, J. Maier, G. Scheffknecht, Corrosion mechanism of alloy 310 austenitic steel beneath NaCl deposit under varying SO_2 concentrations in an oxy-fuel combustion atmosphere, Energy Fuels 27 (2013) 5699-5705. https://doi.org/10.1021/ef4005626.

[27] D. Nordgren, H. Hedman, N. Padban, D. Bostrom, M. Ohman, Ash transformations in pulverised fuel co-combustion of straw and woody biomass, Fuel Process. Technol. 105 (2013) 52-58. https://doi.org/10.1016/j.fuproc.2011.05.027.

[28] Y. Zheng, P.A. Jensen, A.D. Jensen, B. Sander, H. Junker, Ash transformation during co-firing coal and straw, Fuel 86 (2007) 1008-1020. https://doi.org/10.1016/j.fuel.2006.10.008.

[29] A.F. Stam, G. Brem, Fouling in coal-fired boilers: Biomass co-firing, full conversion and use of additives – A thermodynamic approach, Fuel 239 (2019) 1274-1283. https://doi.org/10.1016/j.fuel.2018.11.127.

[30] Y. Liao, S. Wu, T. Chen, Y. Cao, X. Ma, The alkali metal characteristic during biomass combustion with additives, Energy Procedia 75 (2015) 124-129. https://doi.org/10.1016/j.egypro.2015.07.209.

[31] C.W. Bale, E. Belisle, P. Chartrand, S.A. Decterov, G. Eriksson, A.E. Gheribi, et al., FactSage thermochemical software and databases, 2010-2016, Calphad 54 (2016) 35-53. https://doi.org/10.1016/j.calphad.2016.05.002.

[32] B. Zhang. Z. Chang, J. Li, X. Li, Y. Kan, Z. Gao, Effect of kaolin content on the performances of kaolin-hybridized soybean meal-based adhesives for wood composities, Composites Part B: Engineering 173 (2019) 106919. https://doi.org/10.1016/j.compositesb.2019.106919.

[33] ThyssenKrupp Materials International, Material data sheet P22/T22. http://www.s-k-h.com/media/de/service/werkstoffblaetter_englisch/kesselrohre_en/10crmo910_p22_t22_engl.pdf, 2011 (accessed 29 April 2019).

[34] T. Dudziak, T. Hussain, N.J. Simms, High-temperature performance of ferritic steels in fireside corrosion regimes: temperature and deposits, Journal of Materials Engineering and Performance 26 (2016) 84-93. https://doi.org/10.1007/s11665-016-2423-7.

[35] J.N. Harb, E.E. Smith, Fireside corrosion in PC-fired boilers, Prog. Energy Combust. Sci. 16 (1990) 169-90.

[36] A.W. Coats, D.J.A. Dear, and D. Penfold, Phase Studies on the Systems Na_2SO_4–SO_3, K_2SO_4–SO_3, and Na_2SO_4–K_2SO_4–SO_3, J. Inst. Fuel 41 (1968) 129–135.

[37] A.W. Hixson, A.H. Tenney, Chlorine and Salt Cake from Salt and Sulfur, Industrial and Engineering Chemistry 33 (1941) 1472-1484.

[38] A. A. Khan, W. de Jong, P. J. Jansens, H. Spliethoff, Biomass combustion in fluidized bed boilers: Potential problems and remedies, Fuel Process. Technol. 90 (2009) 21-50.

[39] X. Wei, U. Schnell, K. R. G. Hein, Behaviour of gaseous chlorine and alkali metals

during biomass thermal utilisation, Fuel 84 (2005) 841-848

[40] A.J.B Cutler, Corrosion reactions in molten sulphates, Materials Science and Technology 7 (1987) 512-518.

[41] T. Dudziak, T. Hussain, D. Orlicka, A. Pokrywa, N.J. Simms, Fireside corrosion degradation of 15Mo3, T22, T23 and T91 in simulated coal-biomass co-fired environment, Material and Corrosion 66 (2015) 839-850. https://doi.org/10.1002/maco.201407886.

[42] B. Wei, X. Wang, H. Tan, L. Zhang, Y. Wang, Z. Wang, Effect of silicon-aluminum additives on ash fusion and ash mineral conversion of Xinjiang high-sodium coal, Fuel 181 (2016) 1224-1229. https://doi.org/10.1016/j.fuel.2016.02.072.

[43] Y. Wang, Y. Sun, L. Jiang, L. Liu, Y. Li, Characteristics of corrosion related to ash deposition on boiler heating surface during cofiring of coal and biomass, Journal of Chemistry 2020 (2020) 1692598. https://doi.org/10.1155/2020/1692598

[44] L.J. Roberts, P.E. Mason, J.M. Jones, W.F. Gale, A. Williams, A. Hunt, J. Ashman, The impact of aluminosilicate-based additives upon the sintering and melting behaviour of biomass ash, Biomass and Bioenergy 127 (2019) 105284. https://doi.org/10.1016/j.biombioe.2019.105284.

[45] P. Xing, L.I. Darvell, J.M. Jones, L. Ma, M. Pourkashanian, A. Williams, Experimental and theoretical methods for evaluating ash properties of pine and El Cerrejon coal used in co-firing, Fuel 183 (2016) 39-54. https://doi.org/10.1016/j.fuel.2016.06.036.

[46] T.M. Besmann, Thermochemical modeling of refractory corrosion in slagging coal gasifiers, Calphad 32 (2008) 466-469. https://doi.org/10.1016/j.calphad.2008.07.004.